4. Carboxy-Terminated Carbon Nanotube Tips

4.1. Introduction

Scanning tunneling microcopy (STM) has been a powerful tool to study conducting surfaces because of its high spatial resolution.[17] It is, however, often difficult to discriminate functional groups and chemical species. We have recently found that rational chemical modification of STM tips by self-assembled monolayers (SAMs)[25-28] or polypyrrole[29] allows the controlled discrimination of chemical species based on chemical interaction between functional groups on the tip and sample. These chemical selectivities can be ascribed to the facilitated electron tunneling through the overlap of the electronic wave functions of tip and sample formed by chemical interactions, such as hydrogen bond or coordination bond interaction, between chemically modified tips and the samples.[14,25-29] And others also have reported that the attachment of atom/molecule onto STM tip apex enables differentiation of chemical species.[19-23,50,51]

Carbon nanotubes (CNTs) can be regarded as hollow cylinders with diameters of a few nanometers. In spite of their tiny dimensions, they are

mechanically robust and buckle reversibly. In addition, the high electron conductivity of the CNTs is one of the characteristics that makes CNT an attractive material for use as the STM tips, which probe tunneling current flowing to or from sample surfaces. In fact, two research groups have reported that CNT tips allow STM observation to reveal the atomic arrangement of the sample surfaces.[52,53] The CNT tips are also ideal for atomic force microscopy (AFM) and extensively studied to improve spatial resolution of AFM.[54-60] Furthermore, CNTs can be chemically derivatized and functionalized at their ends with various functionalities, as demonstrated in chemical force microscopy with functionalized CNT tips.[61-63] These CNT tips were first prepared by mechanically attaching CNTs on commercial cantilever-tip by acrylic adhesive or amorphous carbon under viewing with an optical microscope or a scanning electron microscope.[52-57,61-63] Recently, it was shown that the CNT tips can also be fabricated by in-situ attachment of CNTs onto AFM tips during the observation[60] or by chemical vapor deposition to directly grow CNTs on AFM tips.[58,59]

We report herein for the first time that the STM tips of single-walled carbon nanotubes (SWNTs), smaller CNTs than multi-walled carbon nanotubes

and thus expected to allow higher resolution, can be prepared by a simple wet chemistry using a reported immobilization procedure of SWNTs onto a flat solid surface;[64,65] carboxylated SWNTs were attached to gold tips coated with SAMs of 4-mercaptobenzoic acid through Zn^{2+} ion bridged coordination in-between.[64] This adds another method to the earlier reported ones[52,53] for the preparation of CNT STM tips. With these SWNT tips, it is demonstrated that the ether oxygens of sample can be selectively and highly reproducibly recognized at high resolution by facilitation of electron tunneling through hydrogen bond interaction between the ether oxygens and carboxyl groups at the apex of SWNTs. The carboxylated SWNT termini are accessible to a variety of covalent chemical modification through amide coupling from the terminal carboxyl groups, to attach molecules having desired functional groups therein.[61-63] Based upon our previous studies,[14,25-29] the results described in this paper may indicate that the rational modification of SWNT tips allow aimed differentiation of chemical species.

4.2. Experimental Section

4.2.1. Reagents.

As-produced SWNT was purchased from Fruuchi Chemicals (Tokyo, Japan) and refluxed for 4 hours in HNO_3[66,67] or ultrasonicated in HNO_3/H_2SO_4 (1/3) for 8 hours.[68] It has been known that both treatments cause segmentation and carboxylation of SWNTs at their terminus.[66-68] The sample diether, 1,11-bis(hexadecyloxy)undecane ($CH_3(CH_2)_{15}O(CH_2)_{11}O(CH_2)_{15}CH_3$), was synthesized as described previously.[26] Deionized water purified with a Milli-Q water system (Japan Millipore, Tokyo, Japan) was used throughout all experiments.

4.2.2. Tip modification.

STM tips were prepared from gold wire (0.25 mm diameter, Nilaco Co., Tokyo, Japan; 99.95 %) by electrochemical etching in 3 M NaCl at AC 10 V. They were washed by sonicating in pure water and further dipping in "piranha solution" (7:3 concentrated H_2SO_4/30% H_2O_2. *Caution: piranha solution reacts violently with organic compounds and should not be stored in closed containers*), finally washed again with pure water. Carboxyl-terminated SWNTs (see above) were immobilized by the three-step procedure as illustrated in Scheme 1. First,

Scheme 1

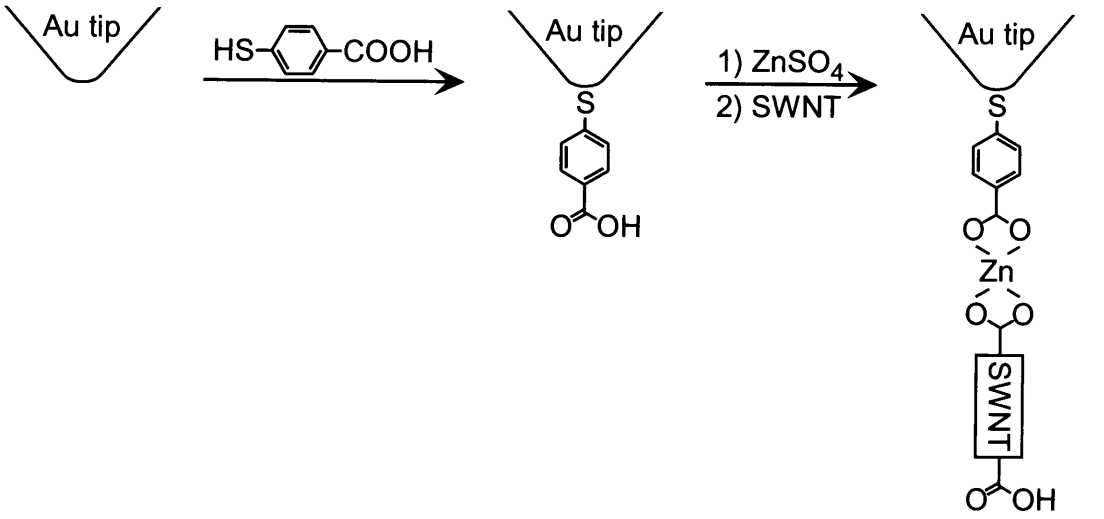

gold STM tips were immersed for more than 12 h in a 1-10 mM ethanolic solution of 4-mercaptobenzoic acid, followed by rinsing them with ethanol and pure water. These tips modified with 4MBA SAMs were dipped in saturated aqueous solution of $ZnSO_4$ for 5 min, and further immersed into the dispersion of the carboxylated SWNTs (about 0.1 mg/mL) for more than 24 h.[64]

4.2.3. STM observation.

STM measurements were performed on a Nanoscope E (Digital Instruments, Santa Barbara, CA). The diether was dissolved in 1,2,4-trichlorobenzene (near saturation), and the resulting solution was applied onto freshly cleaved highly oriented pyrolytic graphite (HOPG; Digital Instruments). Measurements were performed with the constant current mode

under ambient conditions. Typically a bias voltage of varying –0.5 V to –1.0 V (sample negative) and a tunneling current 0.5 – 0.9 nA were employed. No bias dependence was thereby observed. It was also confirmed that no polarity dependence was observed by applying the reversed potential.

4.2.4. Transmission electron microscopy (TEM) observation.

TEM observation was carried out on a HF-2000 (Hitachi, Tokyo, Japan) instrument at optimum defocus with an accelerating voltage of 200 kV. The TEM samples were prepared by gluing the SWNT tips to single hole Cu grid. The care was taken to avoid damage during the observation by minimizing exposure of the sample to the electron beam.

4.3. Results and Discussion

First, we studied the immobilization of SWNTs on STM gold tips by means of TEM. When SWNTs oxidized by ultrasonication in HNO_3/H_2SO_4 were used for the tip modification, we found that not only SWNTs but also the multilayer of aggregated carbon nanoparticles (CNPs) were attached to the tip (Fig. 4.1a). Indeed, it was reported that crude SWNTs thus treated include at

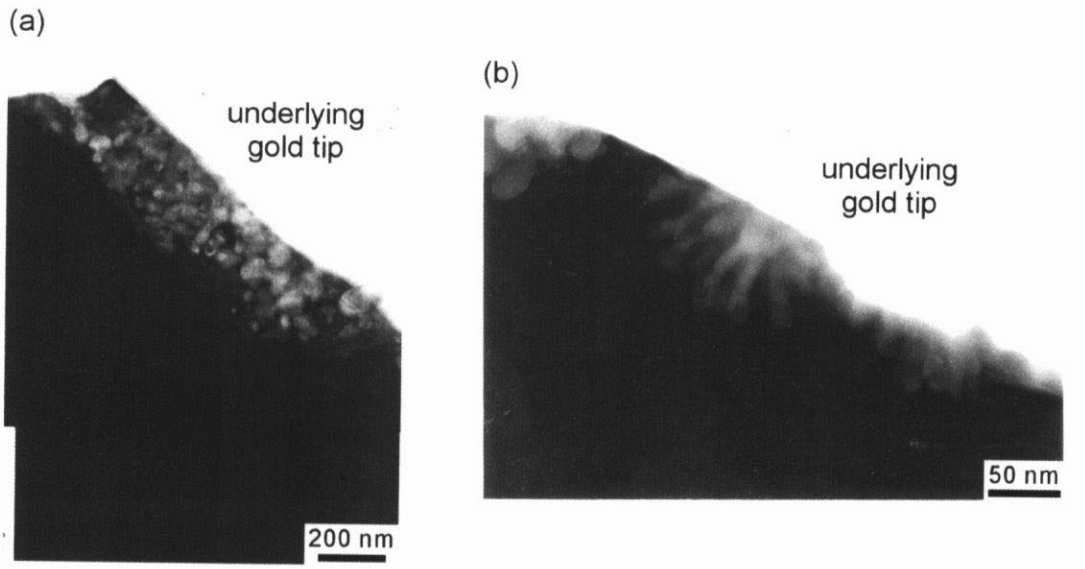

Fig. 4.1. TEM micrographs of STM tips near their apices. (a) Modified with unpurified SWNTs. Aggregated CNPs were immobilized on the underlying gold tip. (b) Modified with purified SWNTs. SWNTs nearly free of CNPs were immobilized on the underlying gold tip. The image was taken near the tip apex marked by the arrow in Inset that shows the whole underlying gold STM tip.

least 1/3 (w / w) of CNPs as impurities.[67] With these "dirty" SWNT tips, we often observed disruptive tunneling current during the STM observation. A most plausible explanation for this unstable tunneling current is desorption of the CNPs in the overlayers during the observation. In contrast, these CNPs were not observed on the tips when SWNTs oxidized by refluxing them in HNO_3 were used (Fig. 4.1b). Instead, SWNT bundles of about 10 nm width were successfully immobilized onto the underlying gold STM tips. The absence of the CNPs in these SWNTs is probably due to favorable oxidative consumption of CNPs over SWNTs during refluxing them in HNO_3.[67] With these "clean" SWNT tips, no disruption of the tunneling current was observed. This result

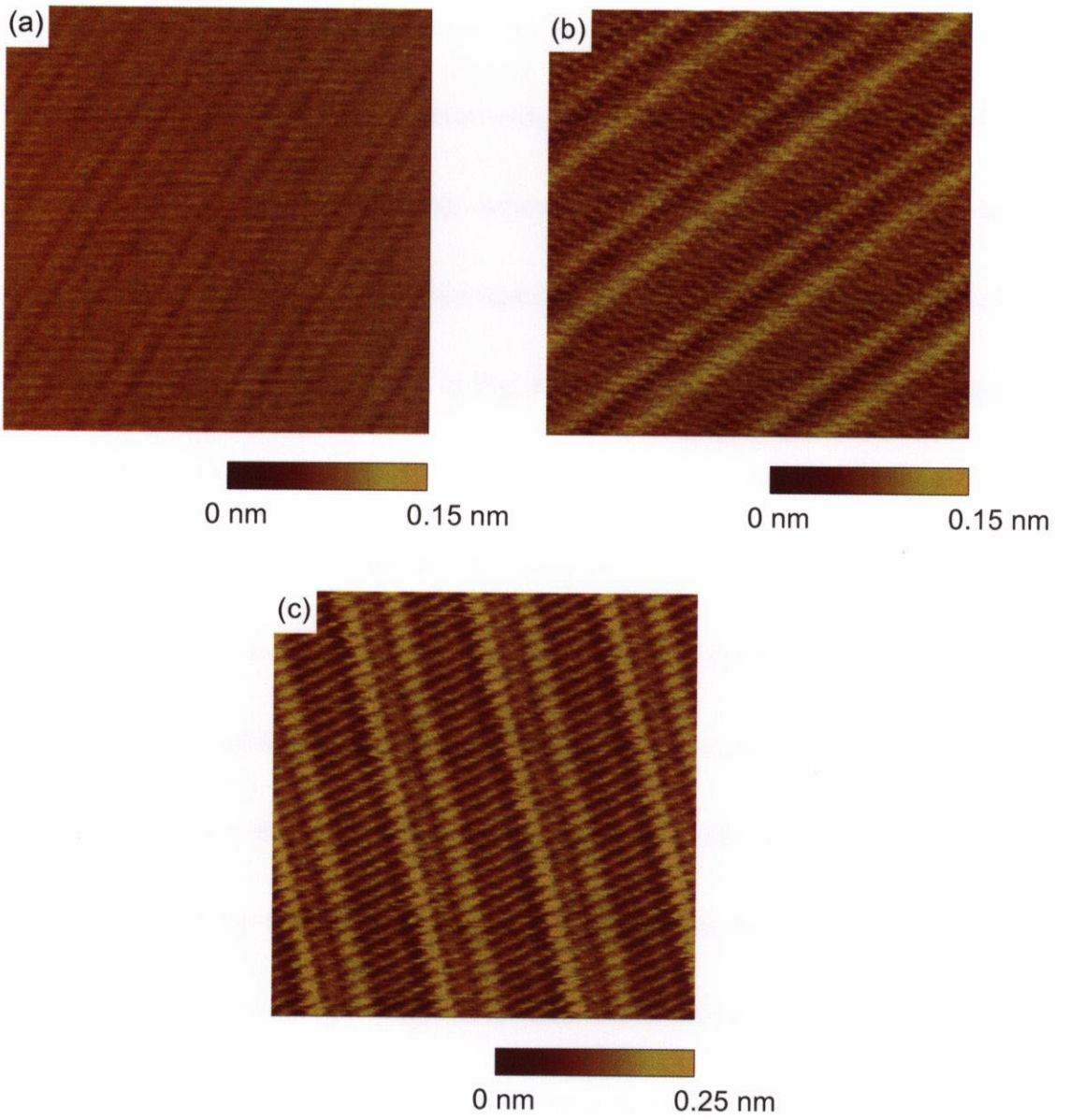

Fig. 4.2. STM images of a diether monolayer physisorbed from a 1,2,4-trichlorobenzene solution onto HOPG. (a) Observed with an unmodified gold tip: sample bias voltage -0.9 V (sample negative) and tunneling current 0.7 nA. (b) Observed with a tip modified with the SAM of 4MBA: sample-bias voltage -1.0 V (sample negative) and tunneling current 0.7 nA. (c) Observed with a SWNT tip: sample-bias voltage -1.0 V and tunneling current 0.4 nA.

shows that the 4MBA/Zn/SWNT assembly fabricated from the solution phases is sufficiently robust for the STM observation.

Fig. 4.2 shows STM images of diether observed with (a) an unmodified

tip, (b) a tip modified with a 4MBA SAM, and (c) an SWNT tip. Pairs of bright lines, which indicate high tunneling conductivity, were observed with 4MBA-modified tips (Fig. 4.2b), whereas these bright lines were absent in images observed with unmodified tips (Fig. 4.2a). We have earlier demonstrated that the pairs of the bright lines in Fig. 4.2b correspond to the two ether oxygens of the diether molecules.[26,27] This change in image contrast selective to the ether oxygens was ascribed to the facilitation of the electron tunneling by hydrogen bond interaction between the ether oxygen of diether and the carboxyl group of 4MBA on the tip. These pairs of bright lines, which reveal the positions of the two ether oxygens of the sample molecules, were observed also with an SWNT tip (Fig. 4.2c). The similarity between the STM images obtained with 4MBA-modified tips (Fig. 4.2b) and those obtained with the SWNT tips (Fig. 4.2c) suggests that the contrast enhancement in Fig. 4.2c also reflects the facilitated electron tunneling by hydrogen bond interaction between the ether oxygens of sample and the carboxyl group at the end of the SWNT. In Fig. 4.2c, individual hydrogen atoms of the methylene groups were resolved in contrast to Fig. 4.2b. The observed result suggests that this SWNT tip gave STM images with an improved chemical selectivity and a higher lateral resolution as

compared with the earlier SAM-modified tip.[25-28] In addition, the corrugation of the sample molecules is more clearly resolved in Fig. 4.2c than in Fig. 4.2b. The small diameters of SWNT or SWNT bundle on the tip are probably responsible for the improved resolution. In general, oxidatively shortened SWNTs have broad distribution of their length as seen in Fig. 4.1b. Because the tunneling current flows only through the foremost part of the probe tip, this heterogeneity guarantees the high resolution achieved in this study even if not an individual SWNT but a larger SWNT bundle is present at the tip apex. The improved resolution would be more advantageous with highly corrugated samples, such as DNAs or proteins.

When tips modified with 4MBA SAMs were used, the number of tips that exhibit the changes in image contrasts for ether oxygens was rather limited (about 24%).[14,26,27] This lack of the contrast enhancement was explained by the removal of a 4MBA molecule from the very apex of the tip during the imaging due to the lateral mobility of the SAM molecules. Because of the exponential dependence on the distance between tip and sample of the tunneling current, the presence of a 4MBA molecule at the very apex of STM tips is a requisite for the contrast enhancement. In contrast, 20 SWNT tips out of

44 examined tips exhibited molecular resolution, and among this, 15 SWNT tips (75%) gave STM images that exhibited selective changes in image contrast of the ether oxygens. The van der Waals interaction between SWNTs is expected to be strong, and is in fact evidenced by their preferential bundle formation as seen in Fig. 4.1b. This strong interaction probably stabilizes the SWNT layer on the underlying SAMs, resulting in the improved reproducibility of the observed contrast change observed in the present study.

SWNT is either metallic or semiconducting depending on its diameter and chiral angle, and of these about two-thirds is reported to be semiconducting. In this study, however, we have not observed the semiconducting behavior of the SWNT tips, such as bias or polarity dependence of the image contrast. This may suggest that not individual SWNTs but SWNT bundles are immobilized onto the underlying gold STM tips and that the bundles show a metallic conductivity because of intertube electronic coupling.[69,70]

The current-voltage characteristics of CNTs are of interest for fundamental understanding of their electronic structures. In principle, scanning tunneling spectroscopy (STS) using CNT tips would allow such a characterization. However, we could not perform reliable STS measurements.

This may be attributed to an unstable and/or insufficient electrical contact at 4MBA/Zn/SWNT interfaces, and this problem is quite common not only to CNT tips for STS but also to almost all applications of CNTs.[53]

4.4. Conclusions

The present study demonstrates that the use of SWNT tips allows chemically selective and highly reproducible STM observation, encouraging us to develop further functionalization of the end of SWNT tip that would tune the chemical selectivity by rationally designing the chemical interactions between SWNT tip and sample. STM observation selective to the metal ion based on coordination bond has been already demonstrated with SAM modified tips.[28] The chemical functionalization of SWNT tips is now in progress for chemically selective imaging based on charge transfer interaction.

5. Control of the Chemical Selectivity

5.1. Introduction

Scanning tunneling microscopy (STM) offers real-space observation with extremely high spatial resolution and has been a powerful tool to study atoms/molecules adsorbed on conducting surfaces [9,11,17]. It is, however, often difficult to discriminate functional groups and chemical species from the conventional STM image contrast. We have recently found that rational chemical modification of STM tips allows chemically selective imaging based upon chemical interactions, such as hydrogen bond [25-27,29,33] or coordination bond interaction [28], between the modified tip and sample [14]. We explained these chemical selectivities on the basis of the facilitated electron tunneling though the overlap of the electronic wave functions by the interaction between tip and sample [14,25-29,33]. Because of its relevance to biological charge-transfer processes, electron transfer by tunneling through hydrogen bonds has attracted considerable attention. The measurement of rate constant for photoinduced electron transfer has shown that electron coupling modulated by hydrogen bonds can be larger than that through σ bonds [30]. With chemically modified

tips, hydroxy, carboxy groups and ether oxygens of monosubstitued hydrocarbons were selectively observed brighter in their STM images due to hydrogen bond facilitated electron tunneling [25-27,29,33]. In these studies, we found that stronger hydrogen bond interaction causes more enhanced contrast for the functional groups [25,29], and the difference in the strength of the hydrogen bond interaction between tip and sample allowed discrimination of the differently oriented ether oxygens [27]. In addition, centers of metal-free porphyrins and porphyrins complexed with Zn(II), Ni(II) were discriminated from each other as differing image contrasts with tips modified with 4-mercaptopyridine (4MP) owing to metal-coordination and hydrogen bond interactions [28].

In the present study, we studied how the differing extent of hydrogen bond acidity or basicity of the tip-modifying molecules affects the selectivity of the observed oxygen-containing functional groups of sample. Four kinds of chemically modified tips and unmodified tips were used for the STM observation of behenic acid 16-hydroxyhexadecyl ester (Fig. 5.1b, abbreviated hereafter as $C_{21}COOC_{16}OH$). SAMs of thiophenol (TP), 4MP, 4-mercaptobenzenesulfonic acid (4MBSA), or 4-mercaptobenzoic acid (4MBA)

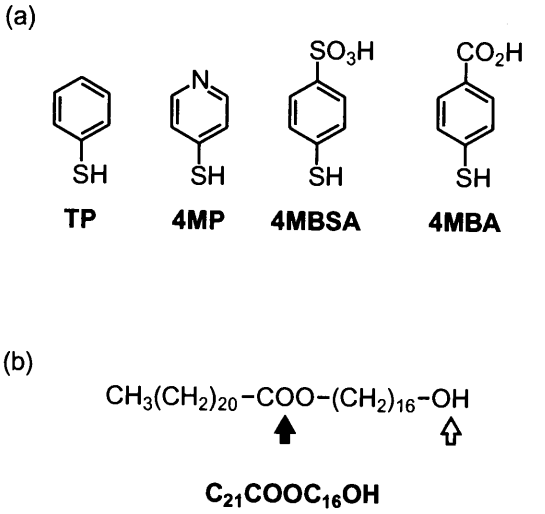

Fig. 5.1. Chemical formulae of the molecules used in the present study along with their abbreviations. (a) Tip-modifying molecules. (b) Sample molecule. The open and close arrows indicate the hydroxy and carboxylate moieties, respectively, to which their discrimination was attained with the tailored modification of the tips by the above tip-modifying molecules.

were immobilized on gold STM tips (Fig. 5.1a). The TP SAMs contain no functional group for hydrogen bond formation, and the 4MP SAMs have a pyridine group, which can work only as a hydrogen bond acceptor. The sulfonyl group of 4MBSA and the carboxy group of 4MBA can form hydrogen bond as donors, but differ in hydrogen bond acidity from each other. With these chemically modified tips, we can control the hydrogen bond acidity or basicity of the tips and strength of the hydrogen bond interactions between the functional groups of the tips and sample molecules.

5.2. Experimental

5.2.1. Reagents

All reagents were used as received and were of the highest grade available. TP and 1,2,4-trichlorobenzene were purchased from Wako Pure Chemical (Osaka, Japan), 4MP and 4MBA were from Tokyo Kasei Kogyo (Tokyo, Japan) and Aldrich Chemical (Milwaukee, USA), respectively. 4MBSA was synthesized from 4-aminobenzenesulfonic acid (Tokyo Kasei Kogyo) according to the reported procedure [71]. De-ionized water purified with a Milli-Q water purification system (Japan Millipore, Tokyo, Japan) was used throughout the experiments. $C_{21}COOC_{16}OH$ was synthesized as follows: Behenic anhydride (1.3 g, 2.0 mmol; Tokyo Kasei Kogyo) was added to a solution of 1,16-hexadecanediol (0.52 g, 2.0 mmol; Wako Pure Chemical), triethylamine (0.5 mL, 3.6 mmol; Wako Pure Chemical), and 4-dimethylaminopyridine (0.042 g, 0.34 mmol; Wako Pure Chemical) in dichloromethane (20 mL). The solution was stirred overnight at room temperature. To the reaction mixture, dichloromethane (80 mL) was added followed by successive washing with 1 M hydrochloric acid and with 2 M aqueous sodium hydroxide. The organic layer was dried over $MgSO_4$, and the solvent was evaporated. The crude product was

purified by multiple column chromatography on silica gel with dichloromethane as eluent. ^{1}H NMR ($CDCl_3$, δ): 0.86 (t, 3H), 1.23 (br 66H), 2.27 (t, 2H), 3.62 (t, 2H), 4.03 (t, 2H).

5.2.2. Tip Preparation

STM tips were prepared from gold wire (0.25 mm diameter, Nilaco Co., Tokyo, Japan; 99.95%) by electrochemical etching in 3 M NaCl at AC 10 V. They were washed by sonicating in pure water and further dipping in "piranha solution" (7:3 concentrated H_2SO_4/30% H_2O_2. *Caution: piranha solution reacts violently with organic compounds and should not be stored in closed containers*) and finally washed again with pure water. SAM formation was carried out by immersion of the Au tips for more than 12 h in a 1–10 mM ethanolic solution of thiol. The modified tips were rinsed with ethanol and pure water prior to use.

5.2.3. STM Observations

STM experiments were carried out on a Nanoscope E (Digital Instruments, Santa Barbara, CA, USA). $C_{21}COOC_{16}OH$ was dissolved in 1,2,4-trichlorobenzene (near saturation), and the resulting solution was applied

onto a freshly cleaved highly oriented pyrolytic graphite (HOPG; Digital Instruments). Observations were performed with a constant current mode under ambient conditions. Typically, a bias voltage of –0.7 to –1.0 V (sample negative) and a tunneling current of 0.5–0.9 nA were employed, and no bias dependence was observed in these bias conditions. We have earlier demonstrated that chemically selective changes in image contrasts (see below) are independent of the imaging condition with a wider range of both bias voltages and tunneling currents [25]. It was also confirmed that the polarity change of bias voltages does not affect the contrast changes although the observed tunneling current is naturally reversed. The absence of the bias and polarity dependence of similar samples was also observed in our previous studies [25-29,33]. Changes in image contrast were observed with at least three tips except for the TP-modified tips, with which no enhanced contrast was observed. Ratio of the tips that exhibited the contrast change (15–30%) was comparable to those in our previous studies with SAMs-modified tips. Also as discussed in our papers, the enhanced contrast often lost upon extending duration of the observation probably due to the lateral movement of the modifying molecules on the tip. We recently found that functionalized carbon

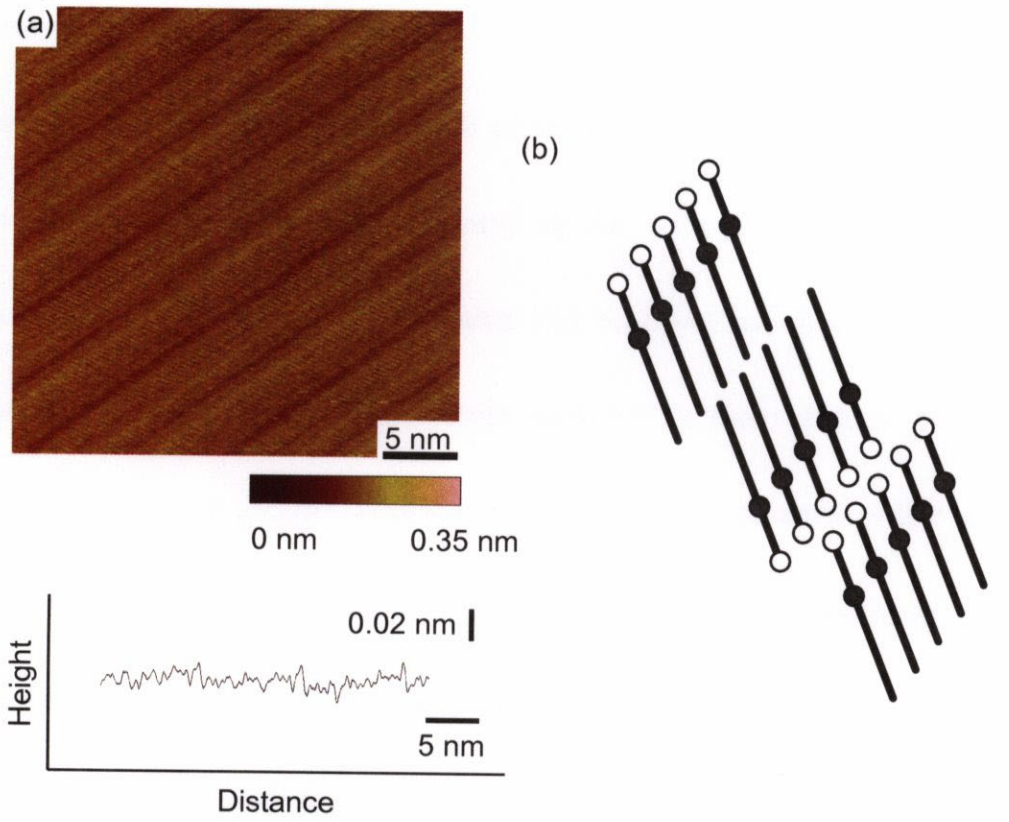

Fig. 5.2. (a) An STM image of $C_{21}COOC_{16}OH$ monolayers physisorbed onto HOPG as observed with an unmodified gold tip, and its averaged cross-sectional profile measured perpendicular to the lamellae: sample bias voltage, 1.0 V (sample negative); tunneling current, 0.5 nA. (b) Schematic illustration of the molecular arrangement for the monolayer of $C_{21}COOC_{16}OH$. Bars represent alkyl chains, and open and closed circles stand for hydroxy and ester groups, respectively.

nanotube STM tips allow more reproducible chemically selective imaging (approximately 75%) [33].

5.3. Results

5.3.1. Unmodified Tips

Fig. 5.2a shows a typical STM image of a $C_{21}COOC_{16}OH$ monolayer

observed with an unmodified gold tip. A lamella structure was seen, and the lamellae were separated from each other by wide and narrow dark lines. The width of the lamellae (5.4 ± 1.4 nm) agrees with the length of the sample molecule estimated from CPK models (5.2 nm), indicating that they consist of the sample molecules, which orient parallel to the substrate surface. The terminal hydroxy groups, which should correspond to either wide or narrow dark lines in Fig. 5.2a, cannot be specified as reported previously [25,29]. The alternate appearance of the wide and narrow dark lines suggests that the sample molecules adsorb onto HOPG with their hydroxy groups head-to-head as illustrated in Fig. 5.2b. No additional distinct bright or dark lines were observed in Fig. 5.2a, and it is consequently difficult to discriminate the carboxylate moieties of $C_{21}COOC_{16}OH$ from the alkyl residues.

5.3.2. 4MP Tips

When 4MP-modified tips were used for the observation of a $C_{21}COOC_{16}OH$ monolayer, parallel bright lines were observed (Fig. 5.3a). They were separated from each other by 11.8 ± 1.8 nm, being close to twice the length of the sample molecules. In the earlier study, we have shown that the

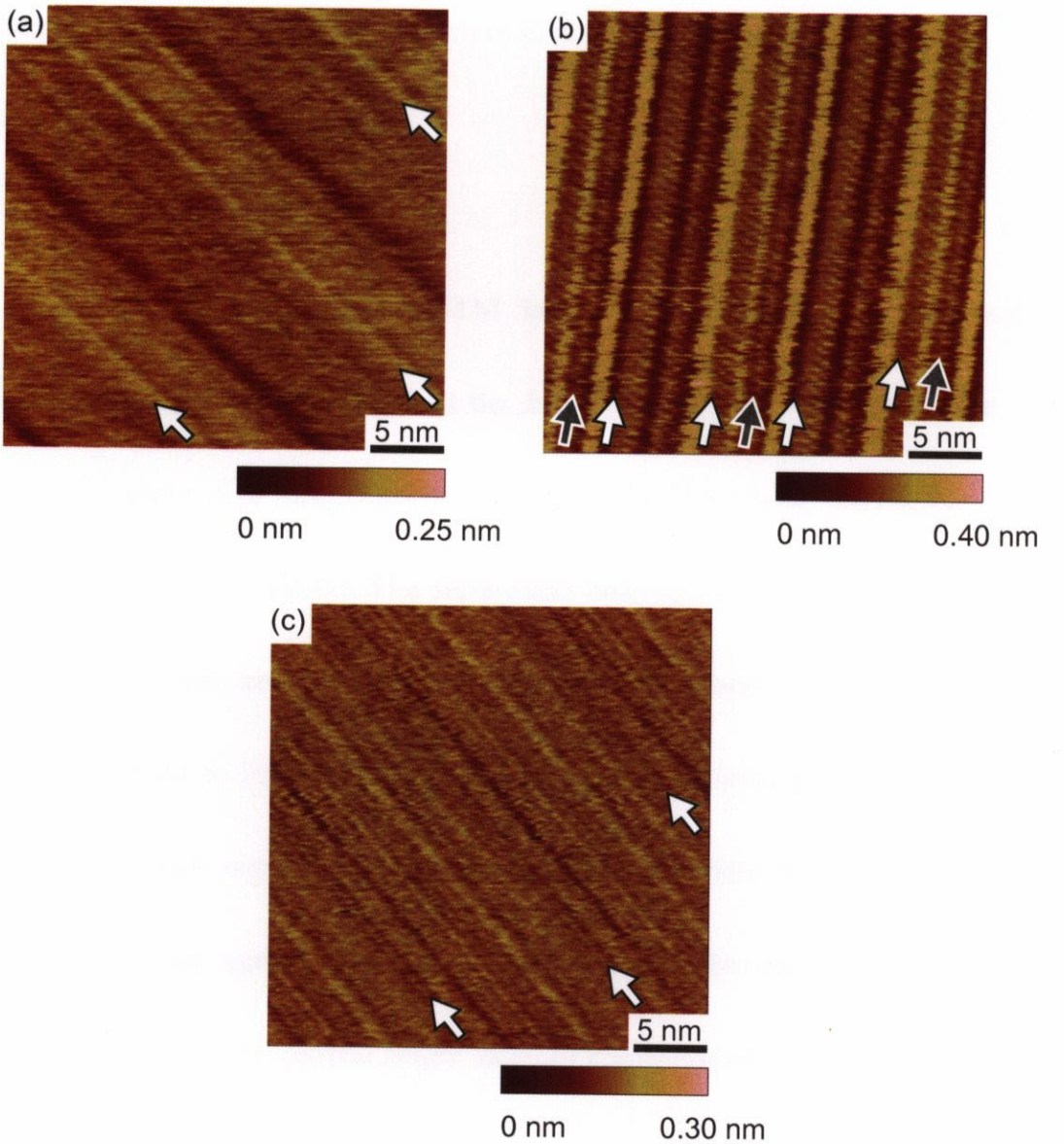

Fig. 5.3. STM images of $C_{21}COOC_{16}OH$ monolayers physisorbed onto HOPG as observed with the molecular tips, and their cross-sectional profiles measured perpendicular to the bright lines: sample bias voltage, 1.0 V (sample negative); tunneling current, 0.5 nA. Arrows point the bright lines that appeared by using chemically modified tips. (a) Observed with 4MP-modified tips. (b) Observed with 4MBSA-modified tips. Open and closed arrows point narrower and wider bright lines, respectively. (c) Observed with 4MBA-modified tips.

4MP-modified tips exhibit the changes in image contrast of the hydroxy groups of 1-octadecanol [25]. Based on the geometrical consistency observed in Fig. 5.3a together with the previous result, it can be concluded that the bright lines reveal

the positions of the hydroxy groups of $C_{21}COOC_{16}OH$.

5.3.3. 4MBSA Tips

Fig. 5.3b presents an STM image of a $C_{21}COOC_{16}OH$ monolayer observed with a 4MBSA-modified tip. In this image, a set of three bright lines, which consists of a single narrower bright line and neighboring two wider bright lines, was observed. The separation between the central and outer lines was 2.8 ± 0.1 nm, and the one between the outer lines was 5.6 ± 0.2 nm. The former is close to 2.4 nm of the length of the hexadecyl group of the sample molecule, which separate the hydroxy and carboxylate moieties. In addition, the latter value agrees with twice the length of the hexadecyl group. The distance between the central bright lines of the neighboring sets of three bright lines was 12.1 ± 0.3 nm, being consistent with twice the length of the sample molecules. Both the symmetry of the three bright lines and their separations conclude that the central narrower bright lines correspond to the hydroxy groups, and the outer two bright lines to the carboxylate moieties of $C_{22}COOC_{16}OH$. The reason for the difference in width of the two kinds of bright line is unclear. This is the first demonstration of the change in image contrast

selective to the carboxylate moiety.

5.3.4. 4MBA-Modified Tips

Next, we used 4MBA-modified tips for the STM observation of $C_{21}COOC_{16}OH$ monolayers. We have recently shown that the 4MBA-modified tips allow selective observation of ether oxygens [26] and discrimination of their orientations [27]. In the STM image of the $C_{21}COOC_{16}OH$ monolayer observed with a 4MBA-modified tip, bright single lines separated by 11.7 ± 1.5 nm from each other were observed (Fig. 5.3c). Like the STM image observed with 4MP-modified tips (Fig. 5.3a), the separation is close to twice the length of the sample molecules. Thus, the bright lines were assigned to the hydroxy groups of the $C_{21}COOC_{16}OH$ molecules. Interestingly, 4MBA-modified tips unlike 4MBSA-modified tips exhibited no discernible bright lines that can be attributed to the presence of the carboxylate.

5.3.5. TP Tips

With TP-modified tips, no change in image contrast was observed at all (data not shown). The STM image observed with TP-modified tips was similar

to those observed with unmodified tips (Fig. 5.2a). The hydroxy groups of $C_{21}COO_{16}OH$ were observed as dark lines and the carboxylate moieties of the ester groups were as bright as the hydrocarbon backbones of the sample molecules.

5.4. Discussion

The sample molecule, $C_{21}COOC_{16}OH$, contains hydroxy and carboxylate moieties, which can form hydrogen bond. They cannot be identified in the STM images observed with either unmodified or TP-modified tips (Fig. 5.2a). The hydroxy groups were observed as dark lines and not capable of being discriminated from the troughs in-between lamellae. No discernible bright or dark image contrast for the carboxylate moiety was observed, making the moiety difficult to be specified in Fig. 5.2a.

When 4MP-modified tips were used, only hydroxy groups were selectively observed as bright lines (Fig. 5.3a). The pyridine nitrogen of the 4MP SAMs on the tip can form hydrogen bonds only with a hydrogen-bond donor, and thus, they can interact only with the hydroxy groups of the sample. The changes in image contrast selective to the hydroxy groups in Fig. 5.3a can be

explained by this selective hydrogen bond interaction with the pyridine of 4MP-SAMs on the tip, which probably enhances tunneling probability [25]. This result clearly shows that the tips modified with hydrogen bond-accepting groups enables selective observation of the functional groups that can work as hydrogen bond donors but not as hydrogen bond acceptors.

Because both the sulfonyl group of 4MBSA and the carboxy group of 4MBA can be acidic functional groups, they can interact with hydrogen bond acceptors. In the STM image of $C_{21}COOC_{16}OH$ observed with 4MBSA-modified tips, a set of three bright lines was observed, revealing both positions of the hydroxy and of the carboxylate moieties of the sample molecules (Fig. 5.3b). In contrast, with 4MBA-modified tips, only a single bright line that corresponds to the hydroxy group was observed. The presence and absence of the contrast enhancement on carboxylate moiety in Fig. 5.3b and in Fig. 5.3c, respectively, can be explained on the basis of the differing extent of the hydrogen bond interaction. Hydrogen bond interactions of the carboxylate moiety are much weaker with the carboxy group of 4MBA-modified tips than with the sulfonyl group of 4MBSA-modified tips, because the hydrogen bond acidity of carboxy groups is in general much lower than that of sulfonyl groups. On the other

hand, hydrogen bond basicity of the hydroxy group is almost the same as that of the carboxylate moiety in nonpolar solvents [72]. However, 4MBA-modified tips gave the contrast change only selective to the hydroxy group. Because the carboxy groups of 4MBA SAMs on the tip can be both of hydrogen-bond acceptor and donor, this result seems to reflect the hydrogen bond acidity of the hydroxy groups. Owing to the acidity, the carboxy group of 4MBA SAMs on the tip is subject to stronger hydrogen bond interaction with the hydroxy group than with the carboxylate moiety in the sample molecule. Hydrogen bond interaction between the carboxy group of 4MBA and the carboxylate moiety of the sample may not be strong enough to enhance the tunneling current. These results indicate chemical selectivity can be controlled by changing the hydrogen bond strength through the design of the tip functionality.

5.5. Conclusions

Chemically modified tips that possess differing degree of hydrogen bonding acidity or basicity were used for the STM observation of $C_{21}COOC_{16}OH$ monolayers. Unmodified and TP-modified tips did not allow the identification of the hydroxy and carboxylate moieties because of the absence of hydrogen

bond functionality on the tips. When 4MP-modified tips were used, the hydroxy groups were selectively observed as bright lines. The pyridine nitrogens can interact with hydroxy groups but not with the carboxylate moiety, hereby enabling the selective detection of hydroxy groups. This result indicates that the modified tips with hydrogen bond acceptors allow selective observation of the hydrogen bond-donating but not -accepting functional groups. Acidic 4MBSA- and 4MBA-modified tips were also used for the STM observation. Whereas 4MBSA-modified tips exhibited the changes in image contrast selective to the both hydroxy and carboxylate moieties of the sample, 4MBA-modified tips allow the contrast change only for the hydroxy groups. The absence of contrast change for the carboxylate moiety with 4MBA-modified tips is due to the weaker hydrogen bond acidity of the carboxy group than that of the sulfonyl group. These results show that upon controlling the extent of the hydrogen bond acidity or basicity of the tip-modifying molecules, the selective observation and discrimination of oxygen-containing functional groups can be tailored.

6. General Conclusions

I have studied on the use of molecular tips for chemically selective STM, which enables detection of intermolecular electron tunneling with high sensitivity and spatial resolution.

In Chapter 3, it is shown that chemical selectivity is attained based on charge-transfer interaction between tip and sample molecules. The chemical recognition arises from facilitation of electron tunneling through the overlap of electronic wave functions brought by the charge-transfer interaction. Based on this and previous works in this laboratory, it is now clear that all of electronic interactions are available for chemically selective observation by molecular tips. The hydrogen bond interaction between tip and sample molecules can be utilized for discrimination of functional groups. The metal-coordination and charge-transfer interactions make it possible to recognize metal ions and electron-donating or -accepting moieties, respectively. The combination of these interactions would allow sophisticated chemical recognition, such as chiral recognition. In addition, it was found that the tunneling current flows in the

direction from the electron-rich porphyrins to the electron-deficient fullerene, but not in the opposite direction. In the present system, the fullerene and porphyrin constitute a tunnel junction, which was regarded as a molecular rectifier. The observed rectification behavior thus suggested that the molecular tips are able to construct a novel intermolecular junction to study molecular conduction in single molecular assembly between tip and substrate related to molecular-scale electronic devices.

Carboxy-terminated carbon nanotubes (CNTs) are utilized for high resolution and chemically selective observation of ether oxygens based on hydrogen bond interaction between carboxy groups at the CNT terminus and the ether oxygens (Chapter 4). The terminal carboxy groups are accessible to a variety of covalent chemical modification through amide coupling to attach molecules having desired functional groups therein.[61-63] Terminally functionalized CNTs would allow high resolutional STM observation with chemical selectivities based on aforementioned three kinds of chemical interactions.

Chapter 5 described that the chemical selectivity can be tuned upon controlling differing extent of hydrogen bond acidity or basicity of tip molecules. This result indicates that molecular tips may allow structural analysis and sequencing of oligosaccharide that is difficult for conventional analytical methodologies. The saccharide contains hydroxy groups, carboxylate moieties, ether oxygens and so forth. Molecular tips enable not only recognition of these functional groups but also discrimination between them.

References

1) Ikai, A. *Surf. Sci. Rep.* **1996**, *26*, 261-332.

2) Tsukada, M.; Kobayashi, K.; Isshiki, N.; Kageshima, H. *Surf. Sci. Rep.* **1991**, *13*, 265-304.

3) Tersoff, J.; Hamann, D. R. *Phys. Rev. Lett.* **1983**, *50*, 1998-2001.

4) Tersoff, J.; Hamann, D. R. *Phys. Rev. B* **1985**, *31*, 805-813.

5) Bardeen, J. *Phys. Rev. Lett.* **1961**, *6*, 57.

6) Lyo, I. W.; Avouris, P. *Science* **1989**, *245*, 1369.

7) Bedrossian, P.; Chen, D. M.; Mortensen, K.; Golovchenko, J. A. *Nature* **1989**, *342*, 258.

8) Chen, C. J. *J. Vac. Sci. Technol. A* **1991**, *9*, 44.

9) Frommer, J. *Angew. Chem., Int. Ed. Engl.* **1992**, *31*, 1298-1328.

10) Cyr, D. M.; Venkataraman, B.; Flynn, G. W. *Chem. Matter.* **1996**, *8*, 1600-1615.

11) Giancarlo, L. C.; Flynn, G. W. *Annu. Rev. Phys. Chem.* **1998**, *49*, 297-336.

12) Giancarlo, L. C.; Flynn, G. W. *Acc. Chem. Res.* **2000**, *33*, 491-501.

13) De Feyter, S.; Gesquiére, A.; Abdel-Mottaleb, M. M.; Grim, P. C. M.; De Schryver, F. C.; Meiners, C.; Sieffert, M.; Valiyaveettil, S.; Müllen, K. *Acc. Chem.*

Res. **2000**, *33*, 520-531.

14) Ito, T.; Umezawa, Y. *Rev. Anal. Chem.* **2000**, *19*, 331-359.

15) Umezawa, Y.; Ito, T. *Electrochemistry* **2003**, *71*, 522-529.

16) Murray, R. W.; Ewing, A. G.; Durst, R. A. *Anal. Chem.* **1987**, *59*, 379A-390A.

17) Wiesendanger, R. *Scanning Probe Microscopy and Spectroscopy: Methods and Applications*; University Press: New York, 1994.

18) Xu, H.; Ng, K. Y. S. *Surf. Sci.* **1996**, *355*, L350-L354.

19) Ruan, L.; Besenbacher, F.; Stensgaard, I.; Laegsgaard, E. *Phys. Rev. Lett.* **1993**, *70*, 4079.

20) Sautet, P.; Dunphy, J. C.; Ogletree, D. F.; Joachim, C.; Salmeron, M. *Surf. Sci.* **1994**, *315*, 127.

21) McIntyre, B. J.; Sautet, P.; Dunphy, J. C.; Salmeron, M.; Somorjai, G. A. *J. Vac. Sci. Technol. B* **1994**, *12*, 1751.

22) Rousset, S.; Gauthier, S.; Siboulet, O.; Sacks, W.; Belin, M.; Klein, J. *Phys. Rev. Lett.* **1989**, *63*, 1265-1268.

23) Bartels, L.; Meyer, G.; Rieder, K.-H. *Appl. Phys. Lett.* **1997**, *71*, 213.

24) McIntyre, B. J.; Slmeron, M.; Somorjai, G. A. *Science* **1994**, *265*, 1415-1418.

25) Ito, T.; Bühlmann, P.; Umezawa, Y. *Anal. Chem.* **1998**, *70*, 255-259.

26) Nishino, T.; Bühlmann, P.; Ito, T.; Umezawa, Y. *Phys. Chem. Chem. Phys.* **2001**, *3*, 1867-1869.

27) Nishino, T.; Bühlmann, P.; Ito, T.; Umezawa, Y. *Surf. Sci.* **2001**, *490*, L579-L584.

28) Ohshiro, T.; Ito, T.; Bühlmann, P.; Umezawa, Y. *Anal. Chem.* **2001**, *73*, 878-883.

29) Ito, T.; Bühlmann, P.; Umezawa, Y. *Anal. Chem.* **1999**, *71*, 1699-1705.

30) de Rege, P. J. F.; Williams, S. A.; Therien, M. J. *Science* **1995**, *269*, 1409-1413.

31) Salomon, A.; Cahen, D.; Lindsay, S.; Tomfohr, J.; Engelkes, V. B.; Frisbie, C. D. *Adv. Mater.* **2003**, *15*, 1881-1890.

32) Carroll, R. L.; Gorman, C. B. *Angew. Chem., Int. Ed. Engl.* **2002**, *41*, 4378-4400.

33) Nishino, T.; Ito, T.; Umezawa, Y. *Anal. Chem.* **2002**, *74*, 4275-4278.

34) Nishino, T.; Ito, T.; Umezawa, Y. *J. Electroanal. Chem.* **2003**, *550-551*, 125-129.

35) Wasielewski, M. R. *Chem. Rev.* **1992**, *92*, 435-461.

36) Imahori, H.; Sakata, Y. *Eur. J. Org. Chem.* **1999**, 2445-2457.

37) Prato, M.; Maggini, M.; Ciacometti, C.; Scorrano, G.; Sandoná, G.; Farnia, G. *Tetrahedron* **1996**, *52*, 5221-5234.

38) Kelly, K. F.; Shon, Y.-S.; Lee, T. R.; Halas, N. J. *J. Phys. Chem. B* **1999**, *103*, 8639-8642.

39) Shon, Y.-S.; Kelly, K. F.; Halas, N. J.; Lee, T. R. *Langmuir* **1999**, *15*, 5329-5332.

40) Mirkin, C. A.; Caldwell, W. B. *Tetrahedron* **1996**, *52*, 5113-5130.

41) Scudiero, L.; Barlow, D. E.; Mazur, U.; Hipps, K. W. *J. Am. Chem. Soc.* **2001**, *123*, 4073-4080.

42) Diederich, F.; Gómez-López, M. *Chem. Soc. Rev.* **1999**, *28*, 263-277.

43) Boyd, P. D. W.; Hodgson, M. C.; Rickard, C. E. F.; Oliver, A. G.; Chaker, L.; Brothers, P. J.; Bolskar, R. D.; Tham, F. S.; Reed, C. A. *J. Am. Chem. Soc.* **1999**, *121*, 10487-10495.

44) Guldi, D. M.; Luo, C.; Prato, M.; Dietel, E.; Hirsch, A. *Chem. Commun.* **2000**, 373-374.

45) Guldi, D. M.; Luo, C.; Prato, M.; Troisi, A.; Zerbetto, F.; Scheloske, M.; Dietel, E.; Bauer, W.; Hirsch, A. *J. Am. Chem. Soc.* **2001**, *123*, 9166-9167.

46) Halas and coworkers reported that a physisorbed C_{60} tip is able to observe electron-scattering patterns around graphite defects of graphite surface, and ascribed it to the electronic configuration of the C_{60} tip that energetically matches scattered electrons (see, for example, *Science* **273**, 1371–1373 (1996)). They demonstrate another ability of fullerene tips, which cannot be recognized with metal tips, though their tip preparation and imaging mechanism is different from those of our fullerene tips.

47) Sun, D.; Tham, F. S.; Reed, C. A.; Chaker, L.; Boyd, P. D. W. *J. Am. Chem. Soc.* **2002**, *124*, 6604-6612.

48) Wang, Y.-B.; Lin, Z. *J. Am. Chem. Soc.* **2003**, *125*, 6072-6073.

49) Aviram, A.; Ratner, M. A. *Chem. Phys. Lett.* **1974**, *29*, 277-283.

50) Bartels, L.; Meyer, G.; Rieder, K.-H. *Surf. Sci.* **1996**, *432*, L621-L626.

51) Xu, Q.-M.; Wan, L.-J.; Yin, S.-X.; Wang, C.; Bai, C.-L. *J. Phys. Chem. B* **2001**, *105*, 10465-10467.

52) Dai, H. J.; Hafner, J. H.; Rinzler, A. G.; Colbert, D. T.; Smalley, R. E. *Nature* **1996**, *384*, 147-150.

53) Shimizu, T.; Tokumoto, H.; Akita, S.; Nakayama, Y. *Surf. Sci.* **2001**, *486*, L455-L460.

54) Wong, S. S.; Harper, J. D.; Lansbury, P. T., Jr.; Lieber, C. M. *J. Am. Chem. Soc.* **1998**, *120*, 603-604.

55) Wong, S. S.; Woolley, A. T.; Odom, T. W.; Huang, J.-L.; Kim, P.; Vezenov, D. V.; Lieber, C. M. *Appl. Phys. Lett.* **1998**, *73*, 3465-3467.

56) Hafner, J. H.; Cheung, C. L.; Lieber, C. M. *Nature* **1999**, *398*, 761-762.

57) Nishijima, H.; Kamo, S.; Akita, S.; Nakayama, Y.; Hohmura, K. I.; Yoshimura, S. H.; Takeyasu, K. *Appl. Phys. Lett.* **1999**, *74*, 4061-4063.

58) Cheung, C. L.; Hafner, J. H.; Odom, T. W.; Kim, K.; Lieber, C. M. *Appl. Phys. Lett.* **2000**, *76*, 3136-3138.

59) Stevens, R.; Nguyen, C.; Cassell, A.; Delzeit, L.; Meyyappan, M.; Han, J. *Appl. Phys. Lett.* **2000**, *77*, 3453-3455.

60) Hafner, J. H.; Cheung, C.-L.; Oosterkamp, T. H.; Lieber, C. M. *J. Phys. Chem. B* **2001**, *105*, 743-746.

61) Wong, S. S.; Joselevich, E.; Woolley, A. T.; Cheung, C. L.; Lieber, C. M. *Nature* **1998**, *394*, 52-55.

62) Wong, S. S.; Woolley, A. T.; Joselevich, E.; Cheung, C. L.; Lieber, C. M. *J. Am. Chem. Soc.* **1998**, *120*, 8557-8558.

63) Wong, S. S.; Woolley, A. T.; Joselevich, E.; Lieber, C. M. *Chem. Phys. Lett.* **1999**, *306*, 219-225.

64) Yu, X.; Mu, T.; Huang, H.; Liu, Z.; Wu, N. *Surf. Sci.* **2000**, *461*, 199-207.

65) Chattopadhyay, D.; Galeska, I.; Papadimitrakopoulos, F. *J. Am. Chem. Soc.* **2001**, *123*, 9451-9452.

66) Tsang, S. C.; Chen, Y. K.; Harris, P. J. F.; Green, M. L. H. *Nature* **1994**, *372*, 159-162.

67) Hiura, H.; Ebbesen, T. W.; Tanigaki, K. *Adv. Mater.* **1995**, *7*, 275-276.

68) Liu, J.; Rinzler, A. G.; Dai, H.; Hafner, J. H.; Bradley, R. K.; Boul, P. J.; Lu, A.; Iverson, T.; Shelimov, K.; Huffman, C. B.; Rodriguez-Macias, F.; Shon, Y.-S.; Lee, T. R.; Colbert, D. T.; Smalley, R. E. *Science* **1998**, *280*, 1253-1256.

69) Kane, C. L.; Mele, E. J.; Lee, R. S.; Fischer, J. E.; Petit, P.; Dai, H.; Thess, A.; Smalley, R. E.; Verschueren, A. R. M.; Tans, S. J.; Dekker, C. *Europhys. Lett.* **1998**, *41*, 683-688.

70) Stahl, H.; Appenzeller, J.; Martel, R.; Avouris, P.; Lengeler, B. *Phys. Rev. Lett.* **2000**, *85*, 5186-5189.

71) Kawai, H.; Sakamoto, F.; Taguchi, M.; Kitamura, M.; Sotomura, M.; Tsukamoto, G. *Chem. Pharm. Bull.* **1991**, *39*, 1422-1425.

72) Abraham, M. H.; Platts, J. A. *J. Org. Chem.* **2001**, *66*, 3484-3491.